SAND2010-1029C

A time-resolved, isomer-resolved study of the propargyl self reaction using a multiplexed photoionization mass spectrometer

David L. Osborn,* Craig A. Taatjes, Fabien Goulay, Talitha M. Selby,† Peng Zou,‡ Askar Fahr§
Combustion Research Facility, MS 9055
Sandia National Laboratories
Livermore, CA 94551-0969

Abstract
The propargyl self reaction ($C_3H_3 + C_3H_3$) is believed to be one of the most important reactions involved in the formation of the first aromatic ring in combustion, a key step on the path to soot formation. In this reaction many isomeric forms of C_6H_6 are energetically feasible (e.g., benzene, fulvene, 1,2 dimethylenecyclobutene, etc.), and the energy landscape that connects them has been explored theoretically. Using multiplexed photoionization mass spectrometry, we have conducted a time-resolved study of this reaction, as a function of pressure at room temperature, to determine which C_6H_6 isomers are formed. We sort isomers based on their distinct ionization energies and Franck-Condon factors for ionization. The experimental data show evidence of a pressure-dependent distribution of many C_6H_6 isomers at 300K. The isomeric branching fractions can be used to place experimental constraints on the height of barriers separating the many wells on this multi-dimensional potential surface. Our apparatus provides the first real-time measurement of different isomers in this chemical reaction, which we compare with multiple well master equation predictions

Introduction
The propargyl radical (H_2CCCH) has long been recognized as a key species in the chemistry of molecular weight growth, the process that converts aliphatic fuels into one- and two-ring aromatic compounds, polycyclic aromatic hydrocarbons, and eventually, soot.[1] The chemistry of soot formation has substantial environmental and human health consequences, and a better understanding of the initial steps in molecular weight growth is needed to produce predictive combustion models.

Although it is a free radical, propargyl is unusually stable, a fact that allows it to attain relatively high concentrations in fuel rich flames. Propargyl's exceptional stability arises for two primary reasons. First, propargyl is a resonance-stabilized free radical. The unpaired electron is delocalized in a π orbital along the carbon backbone of the molecule, with substantial electron density on the CH_2 carbon (knows as the "head" of propargyl), and somewhat lower density on the CH carbon (known as the "tail" of propargyl). An energetic penalty to localize this electron must be paid when propargyl reacts with another molecule, leading to substantially lower reaction rates with O_2 (and all closed-shell molecules) compared to similar reactions of non-resonance-stabilized radicals, such as propyl (C_3H_7). Second, propargyl is sufficiently unsaturated that removal of any of its hydrogen atoms forms highly unstable C_3H_2 species that are either carbenes or diradicals. The high C-H bond strength in propargyl (~ 96 kcal / mol) makes it difficult to oxidize.

In contrast, the reaction of propargyl with itself is a barrierless process[2] with a relatively high rate coefficient of (3.9 ± 0.6) x 10^{-11} cm^3 $molecule^{-1}$ s^{-1} at 296 K .[3] Given the slow reaction of propargyl with stable molecules, and its high concentration compared to other radicals in flames, the propargyl self reaction seems uniquely suited to serve as a significant source of benzene in combustion (and planetary atmospheres) because, atomically at least, it is half of benzene. However, there is no energetically feasible concerted pathway for two propargyl to directly form benzene. Instead, three initial acyclic adducts may be formed when two propargyl radicals react:

$H_2CCCH + H_2CCCH$	$\rightarrow$ $HC{\equiv}CCH_2CH_2C{\equiv}CH$	(1,5-hexadiyne, head-to-head)	(R1)
	$\rightarrow$ $H_2C{=}C{=}CHCH{=}C{=}CH_2$	(1,2,4,5-hexatetraene, tail-to-tail)	(R2)
	$\rightarrow$ $H_2C{=}C{=}CHCH_2C{\equiv}CH$	(hexa-1,2-diene-5-yne, head-to-tail)	(R3)

There have been many investigations of the potential energy surface for this reaction.[4-10] The most complete treatment of the reaction kinetics and product branching ratios comes from the work of Miller and Klippenstein (MK).[2,11] The potential energy surface is characterized by multiple deep potential wells separated by relatively low isomerization barriers.

* Corresponding author: dlosbor@sandia.gov
† Present address: University of Wisconsin, Washington County
‡ Present address: ATMI, Danbury, CT
§ Department of Chemistry, Howard University

The high degree of unsaturation of the C_6H_6 isomers leads to a plethora of isomerization pathways enabled by the uncoupling and recoupling of π electrons. The general reaction mechanism that emerges from these studies is as follows: following association (R1-R3) there is a competition between stabilization due to collisions, isomerization to more stable C_6H_6 isomers, and formation of bimolecular products, driven by the entropy gain this process provides. The three initial adducts (R1 - R3), which are acyclic, non-conjugated molecules lying at ~ -70 kcal/mol with respect to the reactants, can isomerize to form conjugated species (dimethylene cyclobutene and/or ethynyl-substituted 1,3-butadienes) that lie ~ -85 kcal/mol below reactants. These species in turn can undergo ring closure to form the aromatic isomers fulvene (~ -115 kcal/mol) and/or the global minimum isomer, benzene (~ -146 kcal/mol). At sufficiently low pressure or high temperature, isomerization to benzene dominates, and dissociation of benzene to give phenyl (C_6H_5) + H (~ -32 kcal/mol) is the dominant bimolecular exit channel.[11]

Conversely, at sufficiently high pressure and low temperature, collisions stabilize the three initial adducts and prevent further isomerization. At intermediate pressures and temperatures, a wide range of C_6H_6 isomer distributions are predicted, depending sensitively on the enthalpy and entropy of each isomerization transition state that links pairs of wells on the surface.[11] In an environment containing oxygen, the practical ramification resulting from the free energy landscape of C_3H_3 + C_3H_3 is that the initial adducts are fairly easy to oxidize (avoiding the pathways to soot), the conjugated isomers more difficult, and the aromatic isomers the most difficult to oxidize, increasing the likelihood that the more stable C_6H_6 isomers will continue on the pathway toward soot formation. Experiments that probe the C_6H_6 isomer branching fractions are therefore needed to constrain the barrier heights on the potential surface, and such measurements were used, when available, in the validation of MK's reaction mechanism.[11]

The propargyl self reaction has been the subject of many experimental investigations of the kinetics and product branching.[3,12-20] Thermally assisted isomerization of a few individual C_6H_6 isomers also provides information on the barrier heights between wells.[21-26] Whereas the rate coefficient measurements are generally in good agreement, there is less agreement among the isomer branching ratios of C_6H_6. It is a formidable challenge to separate, identify, and quantify the isomers produced in the title reaction. The method chosen in most experiments is gas chromatography / mass spectrometry, although matrix isolation infrared spectroscopy has also been used. To our knowledge, in all cases these isomeric measurements involve end product analysis with a substantial time delay between the reaction and isomeric analysis.

In this paper we present preliminary, time-resolved measurements of the isomeric distributions of C_6H_6 in the propargyl self reaction using Multiplexed Photoionization Mass Spectrometry (MPIMS) at 300 K and pressures of 4 and 8 torr.

Experimental

The MPIMS experiment has been described in detail elsewhere,[27] so only a short description is given here. The apparatus consists of a quartz flow tube in which pulsed laser photolysis creates propargyl radicals at a well-defined time. A small portion of the gas exits through an orifice (400 - 650 μm diameter) in the side of the flow tube, forming a molecular beam that is skimmed before entering the ionization chamber. At a distance of 2.6 cm downstream from the orifice, the molecular beam is crossed by monochromatized synchrotron radiation from the Chemical Dynamics Beamline of the Advanced Light Source synchrotron of Lawrence Berkeley National Laboratory. The synchrotron radiation is used to single-photon ionize neutral species for later analysis by time-resolved mass spectrometry. The radiation is quasi-continuous (500 MHz repetition rate), continuously tunable from 7.3 - 15 eV, with a bandwidth of ~ 30 meV in the present experiments. The photoions enter a miniature double-focusing mass spectrometer of the Mattauch-Herzog design, and are detected in single ion counting mode by a time- and position-sensitive detector. The mass spectrometer simultaneously monitors masses 12 - 120 amu in these experiments.

Propargyl radicals are produced either from the 193 nm photolysis of propargyl chloride (C_3H_3Cl) or the 248 nm photolysis of propargyl bromide (C_3H_3Br), where the laser has an ~ 20 ns pulse width. The precursors are present at mole fractions of ~ 0.01 - 0.03% diluted in helium, with the total pressure in the flow tube either 4 or 8 torr, at a temperature of 300 K. Mass spectra are acquired every 250 μs from 20 ms before to 180 ms after the firing of the photolysis laser.

The resulting ion intensities, $S(m/z, t, E)$, provide a 3-dimensional "image" of the chemical reaction as a function of mass-to-charge ratio (m/z), kinetic reaction time (t), and ionizing photon energy (E). This 3-D data cube can be sliced in several ways to analyze the data, as discussed in the next section. The ability to sort isomers in this time-resolved experiment relies on the fact that each isomer of a particular chemical formula can be identified by its photoionization efficiency curve (ion yield vs. ionizing photon energy). Specifically, the onset of this curve gives the ionization energy of the isomer, and the shape of this curve is determined by the Franck-Condon factors between the neutral and cation state. In principle these two observables form a unique spectral fingerprint for each isomer, allowing us to quantify the isomers present at each (m/z) ratio as a function of time during the reaction. In practice, the propargyl + propargyl system is the most difficult system we have analyzed to date, in terms of the complexity of the (m/z) = 78 (C_6H_6) signals.

Results

Figure 1 shows an overview of a complete 3-D data cube in the C_3H_3 + C_3H_3 reaction, with C_3H_3Cl as the propargyl precursor photolyzed at 193 nm. For each ion (representing a particular neutral molecule) detected, the raw data consists of three values: the *m*/*z* ratio of the ion, its arrival time (50 ns resolution) with respect to the photolysis laser at $t = 0$, and the photon energy E that produced the ion. The raw data is binned into a 3-D $S(m/z, t, E)$ data cube and normalized for variations in the synchrotron radiation flux. Panel (A) shows an $S(m/z, t)$ image sliced from the data cube at $E = 10.2$ eV, where the photolysis laser fires at $t = 0$ ms. This image is summed over reaction time t in panel (C) to give a time-integrated mass spectrum, showing the presence of $m/z = 39$ and 78, which we assign as C_3H_3 and C_6H_6, respectively. Vertical slices can be extracted from the image in panel (A) to show the kinetic time dependence of these two mass peaks in panel (D). In the present work we do not obtain a rate coefficient for the title reaction. However, analysis of the traces in panel (D) shows that C_3H_3 is photolytically produced (with an instrument-limited rise time) and its decay is dominated by 2nd order kinetics, as expected. The temporal rise of C_6H_6 matches the decay of C_3H_3, kinetically linking the product to the reactant.

The image in panel (B) shows a different slice of the 3-D data cube: $S(m/z, E)$ summed from $t = 0$ - 80 ms. This type of slice allows us to identify isomers at each *m*/*z* ratio according to their photoionization efficiency (PIE) spectra. Panel (E) shows two extracted vertical slices from panel (B), which are the total photoionization efficiency curves of C_3H_3 and C_6H_6. Based on this data we conclude that C_3H_3 is exclusively the propargyl (H_2CCCH) isomer, based on its literature ionization energy of 8.67 eV,(reference Chen) and the shape of its PIE curve.(reference Ng) The peaks in the propargyl PIE curve are the result of autoionizing resonances, offering further proof that the isomeric assignment is correct. The main focus of this paper is the quantitative analysis of PIE curves of C_6H_6, as shown in panel (E), which contain contributions from many different isomers. Before analyzing this data, we give some explanations for some other mass peaks observed in Figure 1.

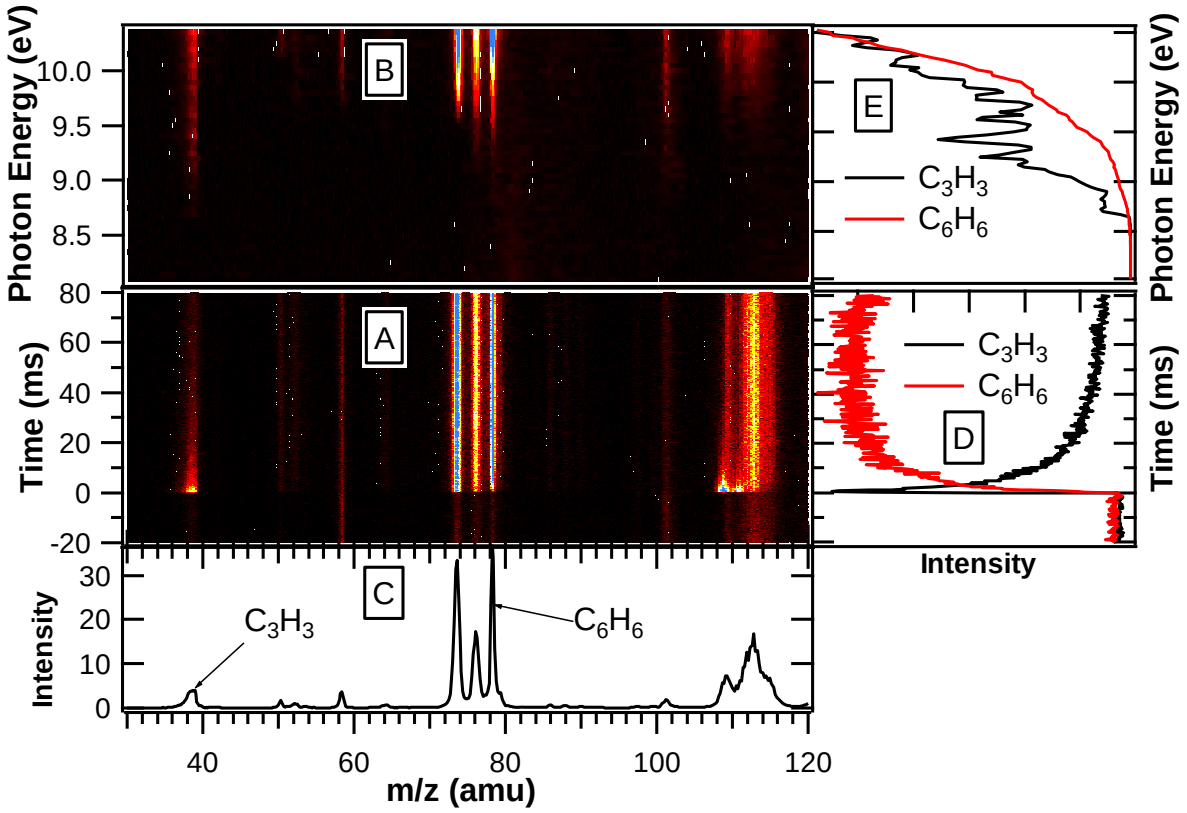

Figure 1. Time-resolved MPIMS images and spectra of the C_3H_3 + C_3H_3 reaction at 4 torr pressure, 300K, with C_3H_3Cl as the precursor. A) Intensity (color scale) as a function of mass and reaction time, detected at 10.2 eV photon energy. B) Intensity as a function of mass and ionizing photon energy, summed over reaction time from 0 - 80 ms. C) Mass spectrum summed over all time and all photon energies. D) Kinetic time traces extracted from image (A). E) Photoionization efficiency curves extracted from image (B).

Two of the strongest peaks not already discussed are m/z = 74 and 76. Mass 74 has an ionization threshold of 9.50 eV, in good agreement with the vertical IE of 9.57 eV[28] for chloroallene ($H_2CCCHCl$). Because of the 3:1 isotopic ratio of ^{35}Cl:^{37}Cl, most of mass 76 is also assigned to chloroallene. There are at least two possibilities for the formation of chloroallene: association of Cl atoms with the tail end of propargyl radicals, and addition of Cl atoms to the tail of propargyl chloride followed by elimination of the Cl atom originally bound to propargyl chloride. The first possibility can be ruled out as a major contributor based on the time trace of m/z = 74, which has a rise time of 1.0 ms. If Cl + propargyl were the source, chloroallene's rise time would be identical to the rise time of C_6H_6 from the propargyl self reaction, because both reactions deplete the propargyl radical population. The much faster rise time of chloroallene argues strongly that it arises from addition-elimination of Cl + propargyl chloride. Because propargyl chloride is present in great excess compared to propargyl radicals, it is reasonable to expect a much faster rate of production of chloroallene via this route than via Cl + propargyl.

If all the m/z = 76 were the ^{37}Cl isotope of chloroallene, its peak height should be 1/3 of m/z = 74 and its PIE curve should be essentially identical to m/z = 74. Instead, there is extra intensity in the mass spectrum at m/z = 76, and the PIE curve shows an additional ionization threshold at 9.00 ± 0.05 eV. This threshold is agrees well with the 9.03 ± 0.05 eV ionization energy of ortho-benzyne (C_6H_4) determined by Zhang and Chen.[29] According to Miller and Klippenstein, benzyne is not expected to be a major bimolecular product of the propargyl self reaction at any pressure or temperature. Its origin in the present experiments is as yet unexplained.

Masses 109 and 111 are assigned to the $CH_2ClCCHCl$ adduct formed when Cl atoms add to propargyl chloride. Within our signal-to-noise, these peaks have the expected 3:2 intensity ratio arising from the ^{35}Cl / ^{37}Cl isotopes in a molecule with two chlorine atoms. Their time profiles are also consistent with a short-lived reactive intermediate expected of this free radical adduct. Additional molecules that can be identified from Figure 1 are diacetylene (m/z = 50, IE = 10.17 eV),[30] and acetone (m/z = 58, IE = 9.70 eV). The origin of time-resolved diacetylene is not clear, although it is a very minor product. Acetone is an impurity from a previous experiment.

Absolute photoionization efficiency spectra of C_6H_6 isomers

In order to extract the relative populations of the C_6H_6 isomers from our data, we require photoionization efficiency spectra with absolute photoionization cross sections of each pure isomer present. To narrow the problem, we consider only the 9 isomers predicted by Miller and Klippenstein to contribute at 300K and pressures from 1 - 10 torr. These isomers are listed in Table 1, along with ionization energies of each isomer. The only isomer with a published absolute photoionization cross section is benzene.[31]

Isomer	Ionization Energy	Pressure = 4 torr		Pressure = 8 torr	
	(eV)	Experimental Fit	Master Equation	Experimental Fit	Master Equation
1,5-hexadiyne	9.94	0.45	0.160	0.55	0.244
1,2,4,5-hexatetraene	8.48	0.004	0.050	0	0.059
dimethylene cyclobutene	8.75	0.006	0.100	0	0.103
fulvene	8.36	0.006	0.114	0.01	0.06
hexa-1,2-diene-5-yne	9.30	0.24	0.424	0.14	0.458
cis 2-ethynyl-1,3-butadiene	8.93	0.12	0.071	0.04	0.038
benzene	9.244	0.15	0.017	0.24	0.005
Cis-1-ethynyl-1,3-butadiene	8.65	0.011	0.036	0.01	0.022
trans-1-ethynyl-1,3-butadiene	8.61	0.007	0.027	0.01	0.012

Table 1. Ionization energies and isomeric branching ratios derived from the fit to the experimental data and from the master equation calculations of Miller and Klippenstein.

We have measured the absolute photoionization efficiency of 1,5-hexadiyne, which is commercially available, by acquiring its PIE spectrum from a sample that also contains a known amount of propene, whose absolute photoionization cross section has been measured by Person and Nicole.[32] The ratio of the two signals, when corrected for the mass discrimination factor in our apparatus[27] and the concentration ratio of the two molecules, yields the absolute cross section

of 1,5-hexadiyne. The remaining isomers are not commercially available, and we have not yet been able to synthesize pure samples of each. Therefore, we calculate their ionization energies, geometries, and force constant matricies using the CBS-QB3 method,[33] which generally provides ionization energies accurate to ± 0.1 eV. The Franck-Condon factors for ionization are calculated, within the harmonic approximation and including the Duschinsky rotation effect for all totally symmetric modes, using the PESCAL program of Ervin.[34] The resulting calculated photoelectron spectra are integrated over electron binding energy to give the relative PIE curve for ionization to the ground state of the cation. The contributions to the PIE curve of excited cation states and autoionizing resonances are not included in these predictions. Finally, each PIE curve is scaled at 11.8 eV to the estimated value of the absolute ionization cross section derived from the semi-empirical method of Bobeldijk et al.[35]

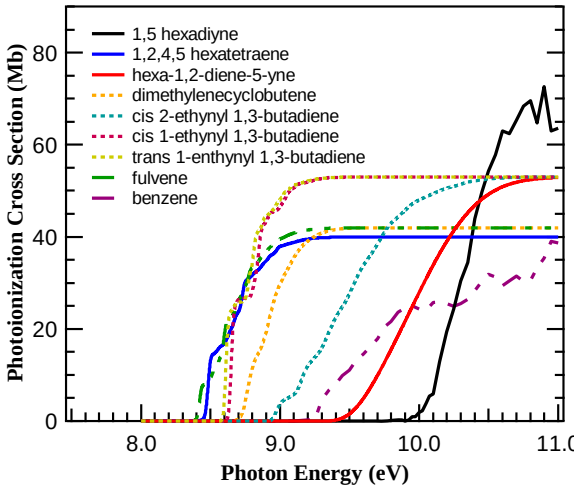

Figure 2. Absolute photoionization efficiency curves of 9 isomers of C_6H_6. Curves are shown for the three initial adducts (solid lines), the four conjugated isomers (dotted lines), and the two aromatic isomers (dash-dot lines).

Figure 2 collects all these PIE spectra with the absolute cross sections given in megabarns (1 Mb = 10^{-18} cm^2 $molecule^{-1}$). The estimated cross sections at 11.8 eV for the two known isomers are 42 Mb (benzene), and 68 Mb (1,5-hexadiyne), in reasonable agreement with the experimentally measured values. Bobeldijk et al. estimate the accuracy of their estimated cross sections as ± 20%. We stress, however, that the use of estimated cross sections and harmonic Franck-Condon factors is non ideal. Our efforts to synthesize, purify, and measure the absolute PIE curves for additional C_6H_6 isomers continue.

Analysis of C_6H_6 photoionization efficiency curves

The total photoionization efficiency curves of C_6H_6 are shown in Figure 3 and Figure 4 at a temperature of 300 K and pressures of 4 and 8 torr, respectively. The total $C_6H_6^+$ signal at any photon energy E can be expressed as follows:

$$S(E) = \sum_{i=1}^{9} \sigma_i(E) n_i$$

where $\sigma_i(E)$ is the absolute photoionization efficiency curve shown in Figure 2 for isomer i, and n_i is the mole fraction of isomer i. The photoionization efficiency curves serve as basis functions in a linear least squares fit to the data with n_i as the parameters. The best fit coefficients are given in Table 1 together with the predicted branching fractions from Miller and Klippenstien. For reference, the total signal $S(E)$ that would be observed using the MK branching fractions is shown as the blue dashed curve. We note that at the temperature and pressures of our experiment, there is no observable change in the isomer distribution evaluated in 10 ms intervals from 0 - 80 ms.

Discussion

Considering the data in Figure 3Figure 4, we can draw a few general conclusions regarding the C_6H_6 isomer distributions. First, as shown in Figure 2, 1,5-hexadiyne has the highest ionization energy of any isomer considered, a large ionization cross section, and a rather steep rise of the PIE above threshold. Examining Figure 3Figure 4, it is clear that the data rises more steeply above 10.0 eV at 8 torr than at 4 torr, implying that the yield of 1,5-hexadiyne is large and increasing with increasing pressure. A second conclusion is that there is relatively little signal below 9.0 eV, which implies there cannot be large populations of isomers with low ionization energies, in particular fulvene and 1,2,4,5-hexatetraene. Although it is not obvious even in the inset of Figure 3, there is a clearly detectable amount of fulvene with a threshold at 8.36 eV, in agreement with the literature value of its ionization energy.[36] Only the isomer with the lowest IE can be detected by itself, leading to exceptional sensitivity for this isomer even if it represents little of the branching fraction. Finally, we note a substantial difference in shape between the predicted total PIE curve from Miller and Klippenstein compared to the data. The master equation results have substantially less 1,5-hexadiyne, and substantially more population of isomers with low ionization energies, in particular, fulvene.

Examining the experimental branching fractions from Table 1, there is some agreement with the trends predicted by Miller and Klippenstein. Most notably, our results agree that 1,5-hexadiyne is a significant product that increases with increasing energy. This result is intuitively pleasing because propargyl has more electron density on the CH2 "head" end, and 1,5-hexadiyne is the head-to-head addition adduct. The tail-tail adduct, 1,2,4,5-hexatetraene , can be formed either by tail to tail addition, or by a Cope rearrangement isomerization from 1,5-hexadiyne. Dimethylene cyclobutene is in turned formed from ring closure of 1,2,4,5-hexatetraene. We see essentially no population of either of these isomers, whereas they represent a total of ~ 15% of the branching in the master equation results. The two rotamers of 1-ethynyl-1,3-butadiene have minor populations in both experiment and the master equation. This result seems mechanistically reasonable because the Miller Klippenstein mechanism predicts that these isomers are created via isomerization of 1,2,4,5-hexatetraene; if there is little of this adduct formed, it is not surprising that 1-ethynyl-1,3-butadiene will also be a very minor product.

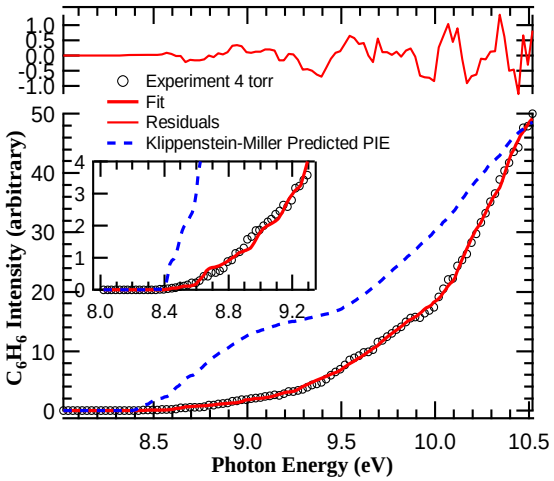

Figure 3. Total photoionization efficiency curve of C_6H_6 (circles) at 4 torr and 300 K. The thick red line represents a fit of the data using the 9 basis functions of Fig. 2. The PIE curve that would result from the populations given by Miller and Klippenstein is shown as the blue dashed curve.

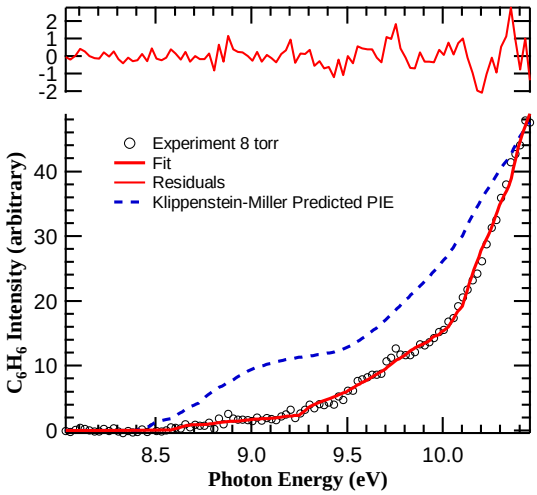

Figure 4. Total photoionization efficiency curve of C_6H_6 (circles) at 8 torr and 300 K. The thick red line represents a fit of the data using the 9 basis functions of Fig. 2. The PIE curve that would result from the populations given by Miller and Klippenstein is shown as the blue dashed curve.

However, our results show some substantial disagreement with the master equation results. First, our experiment shows significant production of the head-to-tail adduct, hexa-1,2-diene-5-yne (24% at 4 torr), but substantially less than the results of MK. Furthermore, it is hard to rationalize why the experiment shows the amount of the head-to-tail adduct decreasing with increasing pressure. Higher pressure should lead to more efficient stabilization into all of the three initial adduct wells.

The most significant discrepancy, however, is the substantial yields of benzene in our fit results. Coupled with the much lower amount of fulvene detected, this result could mean there is a lower energy pathway connecting fulvene to benzene than was found by MK. We note that the pressure dependence of the benzene yield is also somewhat odd, increasing with increasing pressure. However, unlike the case of the head-to-tail adduct's pressure dependence, it is not so easy to rationalize an expected pressure dependence for benzene because there are potentially many pathways leading from the initial adducts to benzene. We note that Howe and Fahr[15] detected a 12% benzene yield at 295 K at a the higher pressure of 20 torr.

There are several sources of uncertainty regarding our experimental fit to the PIE data of C_6H_6 isomers. Foremost is the fact that seven of the nine isomers considered have calculated PIE curves with semi-empirical estimates of their absolute photoionization cross sections. Although the best route to improve the fidelity of the least squares fits would be to have completely experimental absolute cross sections based on pure C_6H_6 isomer samples, this route is a difficult synthetic organic chemistry project. An alternative approach would combine anharmonic calculations of energy levels (and perhaps anharmonic Franck-Condon factors) of multiple cation electronic states (if necessary), coupled with an *ab initio* determination of the ionization cross section. This route it also quite challenging.

It is also reasonable to question the uniqueness of the 9-parameter fit to the experimental data. Further analysis eliminating certain isomers from the fit will give more insight into the consequences of eliminating each isomer. However, it is clear from Figure 3Figure 4 that the C6H6 ion intensity shows a change of slope near 9.25 eV and 10.0 eV. Without adding additional isomers to the fit, it is hard to see how these threshold could be produced without substantial amounts of benzene and 1,5-hexadiyne. Regarding the comparison with Miller and Klippenstein's master equation results, we note that their calculations assume a bath gas of N2, which may have more efficient energy transfer than in our experiments with helium. Furthermore,

for most of the pressure / temperature combinations in MK's analysis, they are in the high pressure limit, lessening the sensitivity to the details of the energy transfer function. However, our low pressure experiments are likely in the fall off regime, where the details of energy transfer may have a larger effect.

Conclusions

We have studied the propargyl self reaction using time-resolved, multiplexed photoionization mass spectometry. In the paper we present a preliminary analysis of the C6H6 isomer distribution at a temperature of 300 K and pressures of 4 and 8 torr. Our results show mixed agreement with the multiple well master equation model of Miller and Klippenstein. Most surprisingly, we observe substantial yields of benzene even at room temperature, in agreement with Howe and Fahr's experimental results, but in disagreement with Miller and Klippenstein. If true, these results, combined with the lack of any appreciable concentration of fulvene and dimethylene cyclobutene, raise the possibility that another pathway from fulvene to benzene may exist with a lower barrier currently mapped pathways. However, we regard this conclusion as speculative at present, due to the uncertainties in the absolute photoionization efficiency spectra used as basis functions in our fit. The most promising path towards a more robust analysis would be the acquisition of experimental absolute PIE spectra for all the isomers considered here. Also valuable would be computational advances for calculating absolute photoionization cross sections of polyatomic molecules, which is by no means an easy task.

Acknowledgements

We thank Mr. Howard Johnsen for excellent technical support during this work. DLO gratefully acknowledges helpful conversations with Drs. James Miller and Stephen Klippenstein and sharing of results prior to publication. This work is supported by the Division of Chemical Sciences, Geosciences, and Biosciences, the Office of Basic Energy Sciences, the U.S. Department of Energy. Sandia is a multiprogram laboratory operated by Sandia Corporation, a Lockheed Martin Company, for the National Nuclear Security Administration under Contract DE-AC04-94-AL85000. The Advanced Light Source is supported by the Direction, Office of Science, Office of Basic Energy Sciences, Materials Science Division, the U.S. Department of Energy under Contract DE-AC02-05CH11231 at Lawrence Berkeley National Laboratory. A.F. acknowledges support of the NASA-Planetary Atmospheres Program (award no. NNG05GQ15G).

[1] H. Bockhorn (Ed.), *Soot Formation in Combusion: Mechanisms and Models*, Springer, New York (1994).
[2] Y. Georgievskii, J. A. Miller, and S. J. Klippenstein, Phys. Chem. Chem. Phys. **9**, 4259 (2007).
[3] J. D. DeSain and C. A. Taatjes, J. Phys. Chem. A **107**, 4843 (2003).
[4] J. A. Miller and C. F. Melius, Combust. Flame. **91** 21 (1992).
[5] C. F. Melius, J. A. Miller, and E. M. Evleth, Proc. Combust. Inst. **24**, 621 (1992).
[6] A. M. Mebel, S. H. Lin, X. M. Yang, and Y. T. Lee, J. Phys. Chem. A **101**, 6781 (1997).
[7] L. K. Madden, A. M. Mebel, M. C. Lin, and C. F. Melius, J. Phys. Org. Chem. **9**, 801 (1996).
[8] A. M. Mebel, M. C. Lin, D. Chakraborty, J. Park, S. H. Lin, Y. T. Lee, J. Chem. Phys. **114**, 8421 (2001).
[9] H. F. Bettinger, P. R. Schreiner, H. F. Schaefer, and P. v. R. Schleyer, J. Am. Chem. Soc. **120**, 5741 (1998).
[10] T. C. Dinadayalane, U. D. Priyakumar, and G. N. Sastry, J. Phys. Chem. A **108**, 11433 (2004).
[11] J. A. Miller and S. J. Klippenstein, J. Phys. Chem. A **107**, 7783 (2003).
[12] U. Alkemade and K. H. Homann, Z. Phys. Chem. Neue Folge **161**, 19 (1989).
[13] S. E. Stein, J. A. Walker, M. M. Suryan, and A. Fahr, Proc. Combust. Inst. **23**, 85 (1990).
[14] A. Fahr and A. Nayak, Int. J. Chem. Kinet. **32**, 118 (2000)
[15] P. T. Howe and A. Fahr, J. Phys. Chem. A **107**, 9603 (2003).
[16] E. V. Shafir, I. R. Slagle, and V. D. Knyazev, J. Phys. Chem. A **107**, 8893 (2003).
[17] B. R. Giri, H. Hippler, M. Olzmann, and A. N. Unterreiner, Phys. Chem. Chem. Phys. **5**, 4641 (2003).
[18] W. Tang, R. S. Tranter, and K. Brezinsky, J. Phys. Chem. A **109**, 6056 (2005).
[19] C. L. Rasmussen, M. S. Skjoth-Rasmussen, A. D. Jensen, and P. Glarborg, Proc. Combust. Inst. **30**, 1023 (2005).
[20] R. X. Fernandes, H. Hippler, and M. Olzmann, Proc. Combust. Inst. **30**, 1033 (2005).
[21] W. D. Huntsman and H. J. Wristers, J. Am. Chem. Soc. **89**, 342 (1967).
[22] H. Hopf, Angew. Chem. **82**, 703 (1970); H. Hopf, Chem. Ber. **104**, 1499 (1971).
[23] R. S. Tranter, W. Tang, K. B. Anderson, and K. Brezinsky, J. Phys. Chem. A **108**, 3406 (2004).
[24] K. B. Anderson, R. S. Tranter, W. Tang, K. Brezinsky, and L. B. Harding, J. Phys. Chem. A **108**, 3403 (2004).
[25] C. H. Miller, W. Tang, R. S. Tranter, and K. Brezinsky, J. Phys. Chem. A **110**, 3605 (2006).

[26] W. Tang, R. S. Tranter, and K. Brezinsky, J. Phys. Chem. A **110**, 2165 (2006).
[27] D. L. Osborn, P. Zou, H. Johnsen, C. C. Hayden, C. A. Taatjes, V. D. Knyazev, S. W. North, D. S. Peterka, M. Ahmed, and S. R. Leone, Rev. Sci. Instrum. **79**, 104103 (2008).
[28] J. Kroner, W. Kosbahn, and W. Runge, Ber. Bunsen-Ges. Phys. Chem. **81**, 826 (1977).
[29] X. Zhang and P. Chen, J. Am. Chem. Soc. **114**, 3147 (1992).
[30] G. Bieri, A. Schmelzer, L. Asbrink, and M. Jonsson, Chem. Phys. **49**, 213 (1980).
[31] T. A. Cool, J. Wang, K. Nakajima, C. A. Taatjes, and A. McIlroy, Int. J. Mass Spectrom. **247**, 18 (2005).
[32] J. C. Person, P. P. Nicole, J. Chem. Phys. **53**, 1767 (1970).
[33] J. A. Montgomery, M. J. Frisch, J. W. Ochterski, and G. A. Petersson, J. Chem. Phys. **112**, 6532 (2000).
[34] K. M. Ervin, Fortran program PESCAL, University of Nevada, Reno, 2004.
[35] M. Bobeldijk, W. J. van der Zande, and P. G. Kistemaker, Chem. Phys. **179**, 125 (1994).
[36] G. Bieri, F. Burger, E. Heilbronner, and J. P. Maier, Helv. Chim. Acta, **60**, 2213 (1977).